

Effect of Carbon Content on Cracking Phenomenon Occurring during Cold Rolling of Three Light-Weight Steel Plates

SEUNG YOUB HAN, SANG YONG SHIN, SUNGHAK LEE, NACK J. KIM, JAI-HYUN KWAK, and KWANG-GEUN CHIN

Effects of carbon content on cracking phenomenon, which often occurred in cold-rolled light-weight steel plates, were investigated in this study. Three steels were fabricated by varying carbon content, and their microstructures and tensile properties were investigated. The steel containing low carbon content of 0.1 wt pct consisted of thin κ -carbide bands, coarse band boundary κ -carbides, and ferrites. As the carbon content increased, volume fractions of κ -carbide bands and total κ -carbides increased, and band boundary κ -carbides were finely distributed in relatively wide band boundary areas. Microstructural observation of the deformed region of tensile specimens revealed that coarse κ -carbides continuously formed along band boundaries worked to initiate the cracking or to facilitate the abrupt crack propagation into ferrites or band boundaries in a cleavage fracture mode, while bands densely populated with fine, lamellar κ -carbides did not play a critical role in the cracking. Thus, the increase in carbon content effectively minimized the formation of band boundary carbides and reduced their size, thereby resulting in the prevention of cracking during cold rolling and in the simultaneous improvement of ductility and strength.

DOI: 10.1007/s11661-010-0456-3

© The Minerals, Metals & Materials Society and ASM International 2010

I. INTRODUCTION

MANY efforts to reduce the weight of steel plates in automotive industries have been conducted in order to increase fuel efficiency and to decrease CO₂ emissions.^[1–8] In addition to light weight needs, automotive steels require excellent strength to sustain automotive structures and to reduce the impact or shock in cases of accidents. Thus, highly deformable steel plates such as transformation induced plasticity (TRIP) steels and twinning induced plasticity (TWIP) steels have been actively developed.^[1–5,8–12] Recently, a large amount of Mn and Al has been added to automotive steels to achieve the light-weight effect as well as excellent strength and ductility, and their total amounts are generally larger than 15 wt pct. This addition leads to about 10 wt pct reduction in comparison with TRIP or TWIP steels, and often offers excellent properties such as strengths of over 780 MPa and elongations of over 30 pct.^[9–15]

Alloying elements used for light-weight steels mainly include Mn, Al, and C because the decreased specific gravity due to substitutional or interstitial atoms works to reduce the weight.^[16–19] Mn raises the volume fraction of austenite at high temperatures as an austenite stabilizer, but the increased Mn content often leads to the formation of a large amount of ferrite during cooling.^[20] It also poses problems such as increased manufacturing costs and deteriorated productivity, because the temperature of the steel melt can be lowered during the steel-making process. Thus, efforts to reduce the Mn content in the light-weight steels have been made. Aluminum, a ferrite stabilizer, helps form a dual-phase structure of ferrite and austenite at high temperatures and promotes the precipitation during cooling.^[16–18] When the steels contain hardenability elements such as C, precipitates such as carbides or nitrides are well formed, and the amount of precipitates varies with contents of Mn and Al as well as C.^[16–18] According to these precipitates, the steels are often exposed to the cracking occurring during cold rolling.

The light-weight steels containing about 10 wt pct of Mn and Al are newly developed, but their detailed microstructures or deformation and fracture mechanisms are hardly known. Furthermore, very few studies on the systematical explanation of the cracking phenomenon of cold-rolled steel plates have been conducted, although some studies related with textures and the segregation of precipitates were reported.^[21–25] In the present study, therefore, three cold-rolled light-weight steel plates having different carbon content were fabricated, and the cracking phenomenon occurring during cold rolling was clarified in relation with microstructural parameters including precipitates.

SEUNG YOUB HAN, Research Assistant, SANG YONG SHIN, Research Professor, and SUNGHAK LEE, Professor, are with the Center for Advanced Aerospace Materials and the Materials Science and Engineering Department, Pohang University of Science and Technology, Pohang 790-784, Korea. Contact e-mail: shlee@postech.ac.kr NACK J. KIM, Professor, is with the Graduate Institute of Ferrous Technology and the Center for Advanced Aerospace Materials, Pohang University of Science and Technology. JAI-HYUN KWAK, Senior Principal, Sheet Products & Process Research Group, and KWANG-GEUN CHIN, Steel Research Project Team, TWIP Steel Research Project Team, are with the Technical Research Laboratories, POSCO, Kwangyang, 545-090, Korea.

Manuscript submitted April 9, 2010.

Article published online October 19, 2010

The primary causes for the cracking were analyzed by the detailed microstructural examination, and methods to prevent or minimize the cracking were suggested.

II. EXPERIMENTAL

A. Light-Weight Steels

Three light-weight steels were fabricated by a vacuum induction melting method, and their chemical compositions are shown in Table I. The steels containing carbon content of 0.1, 0.2, and 0.3 wt pct are referred to as “C1,” “C2,” and “C3,” respectively, for convenience. The rolling conditions are shown in Figure 1. After thick plates of 160 mm in thickness were homogenized at 1473 K (1200 °C) for 1 hour, they were hot rolled at 1453 K (1180 °C), and the rolling was finished at 1173 K (900 °C). They were then cooled in a furnace from 923 K (650 °C) after holding at this temperature for 1 hour. The hot-rolled steel plates of 3 mm in thickness were rolled at room temperature to make 2-mm-thick steel plates. Most of the C1 steel plates were cracked during the initial stage of cold rolling, whereas the C3 steel plates were not cracked during cold rolling. Only a few C2 steel plates were cracked.

B. Microstructural Analysis

The steels were polished and etched in a 2 pct nital solution, and microstructures of longitudinal-transverse

Table I. Chemical Compositions of the Light-Weight Steels (Weight Percent)

Steel	C	Mn	Al	P	S
C1	0.1	4 to 6	6 to 8	<0.01	<0.01
C2	0.2				
C3	0.3				

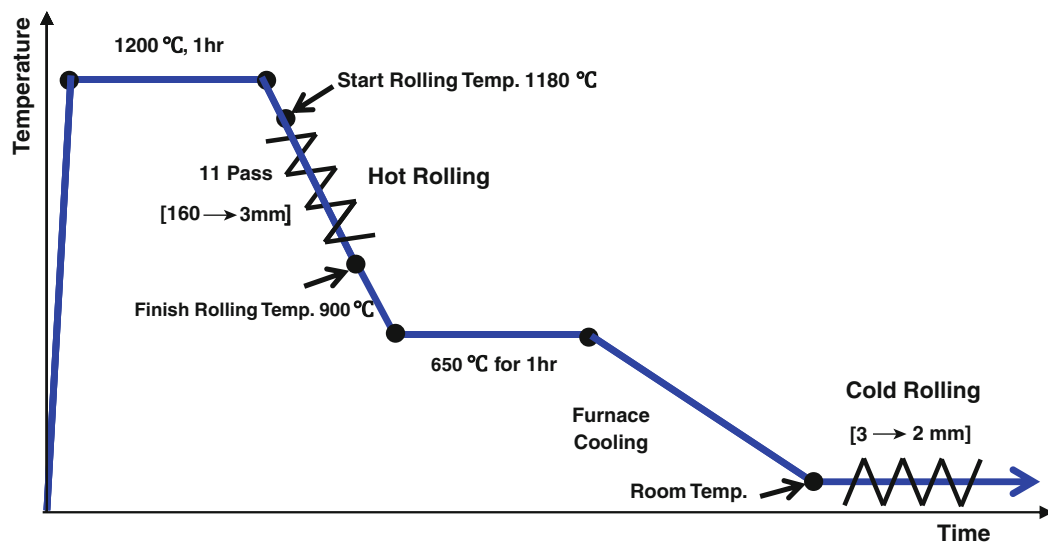


Fig. 1—Schematic illustration of rolling conditions for the light-weight steel plates.

(L-T) planes were observed by an optical microscope and a scanning electron microscope (model: JSM-6330F, JEOL*). Phases present in the steels were

*JEOL is a trademark of Japan Electron Optics Ltd., Tokyo.

identified by X-ray diffraction (XRD) and transmission electron microscopy (TEM), and their volume fractions were measured by an image analyzer (model: SigmaScan Pro, ver. 4.0, Jandel Scientific Co., San Rafael, CA). For the TEM observation, specimens were mechanically polished to a thickness of 50 μm , punched to prepare disc specimens (3-mm diameter) by a disc cutter, and then ion milled to prepare thin foil specimens. The thin foils were observed by a transmission electron microscope (model: 2100, JEOL) operated at an acceleration voltage of 200 kV. Hardness of phases and overall bulk hardness were measured by a Vickers hardness tester under 50 and 300 g loads, respectively.

C. Tensile Test

Tensile specimens were obtained from the $\frac{1}{2}$ thickness location of the cold-rolled plate. Plate-type tensile specimens having a gage length of 12.6 mm, gage width of 5 mm, and gage thickness of 1 mm were prepared in the transverse direction, and were tested at room temperature at a strain rate of 10^{-3} /s by a universal testing machine of 100 kN capacity (model: 5582, INSTRON**). In order

**INSTRON is a trademark of Special Metals Corporation, New Hartford, NY.

to investigate the crack initiation and propagation processes, the fracture surface and the cross-sectional area beneath the fracture surface were observed by scanning electron microscopy (SEM).

III. RESULTS

A. Microstructure

Optical micrographs of the cold-rolled C1, C2, and C3 steels are shown in Figures 2(a) through (c). All the microstructures are parallel to the rolling direction in a banded shape and are almost similar to those of hot-rolled steel plates, although the band structure is

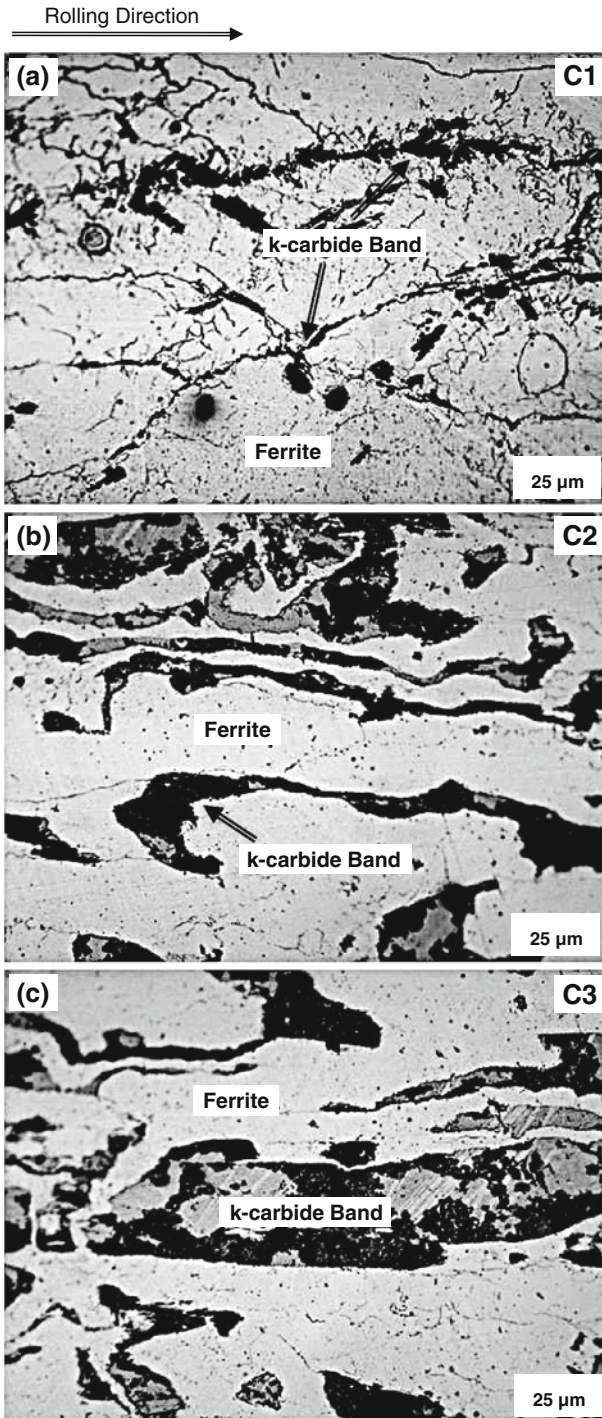


Fig. 2—Optical micrographs (L-T plane) of the (a) C1, (b) C2, and (c) C3 steels. Nital etched.

somewhat more severely formed in the cold-rolled steel plates. Dark-colored bands in the C1 steel are very thin, and the thickness of the bands increases in the order of the C1, C2, and C3 steels. These dark-colored bands contain a number of secondary phases, and the volume fraction of secondary phase bands tends to increase with increasing carbon content in the steels.

X-ray diffraction pattern of the C3 steel is provided in Figure 3. Peaks of ferrite and κ -carbides are observed. Figures 4(a) through (c) show TEM bright-field image, diffraction pattern, and pattern analysis diagram, respectively, for lamellar-shaped secondary phases formed the secondary phase band. According to the calculation of crystal structure and lattice parameter, the secondary phase is identified to be a κ -carbide of a perovskite structure with lattice parameter of 3.80 Å. The lattice parameter of κ -carbides changes in the range of 3.7 to 3.8 Å, because it varies slightly with the aluminum content contained inside κ -carbides.^[26,27] Since κ -carbides precipitated from austenite are coherent with the matrix in general, ferrites and κ -carbides nucleated in austenite have a Nishiyama–Wasserman orientation relationship. Thus, secondary phases present in the C1 through C3 steels (Figures 2(a) through (c)) are κ -carbides, and thus dark-colored secondary phase bands are referred to as κ -carbide bands.

Detailed SEM micrographs of the κ -carbide bands of the C1 and C3 steels are shown in Figures 5(a) through (d). The C1 steel consists of κ -carbide bands and κ -carbides coarsely formed along band boundaries, as indicated by the white arrows in Figure 5(a). Between these bands, equiaxed ferrite grains of 3 to 10 μm in size are found. The higher-magnification SEM micrograph of the κ -carbide band area is shown in Figure 5(b). Fine, lamellar κ -carbides are densely distributed in the ferrite matrix inside the κ -carbide band, and their thickness and the interspacing between them are very small. Coarse, spherical κ -carbides of 0.3 to 0.8 μm in size are observed in the band boundary area (Figures 5(a) and (b)). In the C3 steel, κ -carbide bands are well developed, and their thickness is much larger than that of the C1 steel (Figure 5(c)). Equiaxed ferrite grains of 5 to 10 μm in size are placed between bands, as indicated by white arrows. Inside the κ -carbide band, fine, lamellar κ -carbides exist in the ferrite matrix, such as in the C1 steel, but their thickness and the interspacing between them are larger than those of the C1 steel (Figure 5(d)).

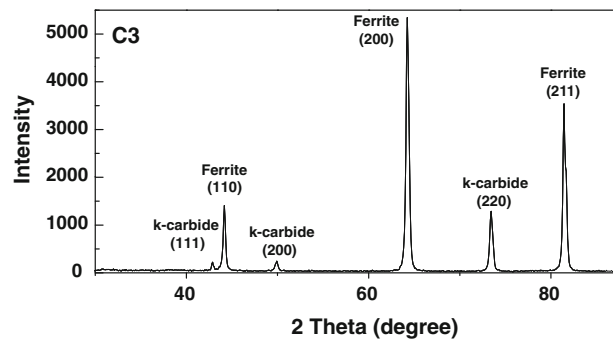


Fig. 3—XRD results of the C3 steel.

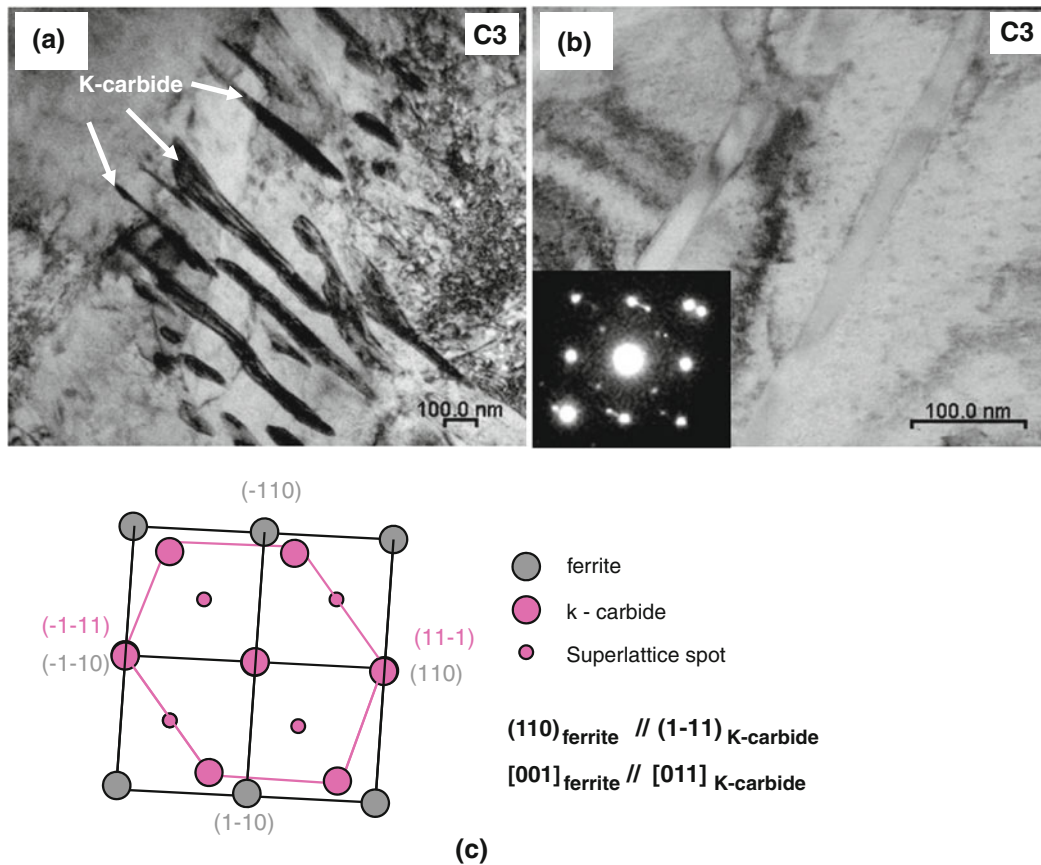


Fig. 4—(a) TEM bright image, (b) selected area diffraction (SAD) pattern, and (c) analysis of SAD pattern of κ -carbides in the C3 steel.

Fine, spherical κ -carbides of about $0.1 \mu\text{m}$ in size are found in the band boundary area.

Volume fractions of ferrite area, κ -carbide band, and band boundary κ -carbides, together with thickness of the κ -carbide band, are summarized in Table II. The volume fraction and thickness of κ -carbide bands are about 8 pct and $6.5 \mu\text{m}$, respectively, in the C1 steel, and increase in the order of the C2 and C3 steels with increasing carbon content. The volume fraction of band boundary κ -carbides in the C1 steel is about 3.2 pct, which is much higher than that of the C2 and C3 steels.

B. Hardness and Tensile Properties

The Vickers hardness of ferrite area and κ -carbide band and the overall bulk hardness are listed in Table III. The hardness of the ferrite area is 214 VHN in the C1 steel and increases up to 274 VHN in the C3 steel with increasing carbon content, whereas the hardness of the κ -carbide band is similar at about 250 VHN in the three steels. The overall bulk hardness increases in the order of the C1, C2, and C3 steels and shows the same trend of the ferrite hardness.

Figure 6 shows room-temperature tensile stress-strain curves, from which tensile properties are summarized in Table IV. The elongations of the three steels are less than 3 pct in a cold-rolled plate state. All the steels show a continuous yielding behavior, and both the yield and

ultimate tensile strengths increase with increasing carbon content. This is because the volume fraction of κ -carbide bands increases in the order of the C1, C2, and C3 steels. The elongation of the C2 and C3 steels is 2.6 pct, which is 3 times higher than that of the C1 steel. Both the strength and ductility of the C1 steel are quite low.

Figures 7(a) through (c) show SEM micrographs of the cross-sectional area beneath the fracture surface of the C1 and C3 steels. Here, the rolling direction and tensile loading direction are perpendicular. Several cracks are observed in the C1 steel, and most of them are initiated at κ -carbide band boundaries (Figure 7(a)). Since coarse κ -carbides are placed continuously along band boundaries, they are readily cracked. Some band boundaries are largely separated to form long and wide cracks as indicated by arrows. Microcracks are observed inside the κ -carbide band, but the number of microcracks is few as fine, lamellar κ -carbides are densely distributed inside the κ -carbide band (Figure 5(b)). Thus, band boundary κ -carbides work as main crack initiation sites, and cracks rapidly propagate into ferrites or along band boundaries in a cleavage fracture type (Figure 7(b)). It is not likely that a few microcracks initiated inside the band affect the overall cracking behavior, although some cracks propagate into the band. In the C3 steels, on the other hand, cracks initiate mainly inside the κ -carbide band, but do not seem to grow to form long cracks (Figure 7(c)). Band

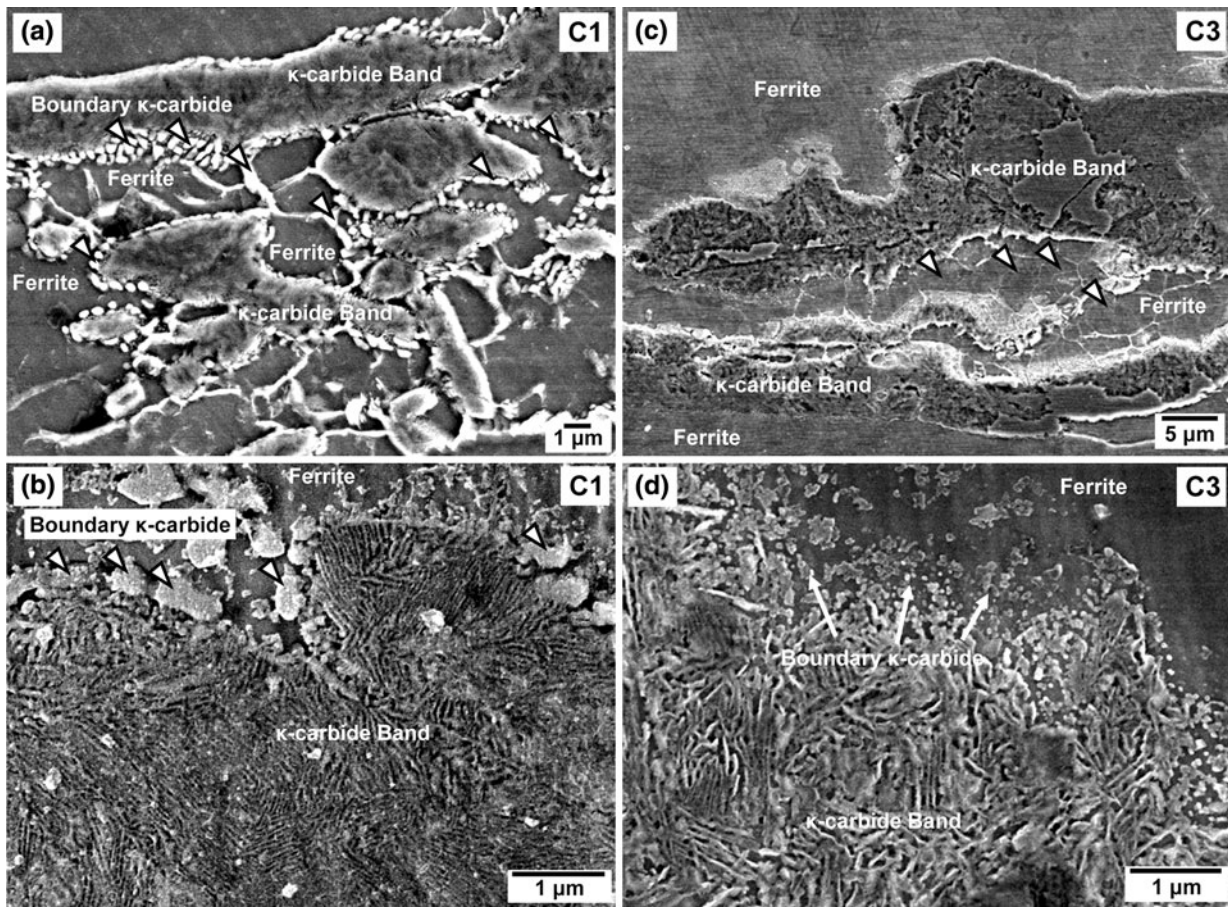


Fig. 5—SEM micrographs (L-T plane) of the (a) and (b) C1 and (c) and (d) C3 steels. Nital etched.

Table II. Volume Fractions of Ferrite Area, κ -Carbide Band, and Band Boundary κ -Carbides, and Thickness of κ -Carbide Band

Steel	Volume Fraction (Pct)			Thickness of κ -Carbide Band (μm)
	Ferrite Area	κ -Carbide Band	Band Boundary κ -Carbide	
C1	balance	8.3 ± 2.4	3.2 ± 0.8	6.5 ± 3.4
C2	balance	17.4 ± 3.8	1.2 ± 0.7	25.7 ± 11.0
C3	balance	26.6 ± 6.1	0.9 ± 0.2	31.1 ± 18.5

Table III. Vickers Hardness Test Results of the Light-Weight Steels (VHN)

Steel	Ferrite Area	κ -Carbide Band	Overall Hardness
C1	214 ± 11	248 ± 10	221 ± 19
C2	246 ± 13	256 ± 16	252 ± 17
C3	274 ± 21	255 ± 19	265 ± 25

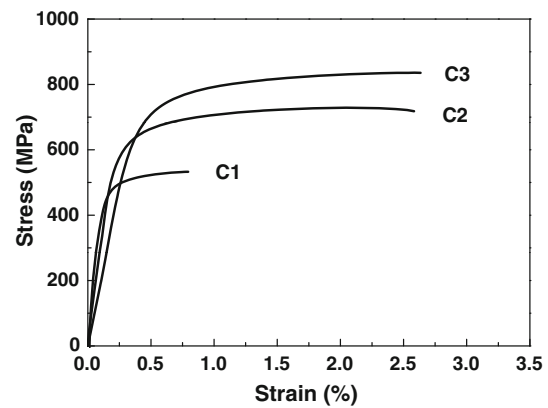


Fig. 6—Room-temperature tensile stress-strain curves of the steels.

Table IV. Room-Temperature Tensile Test Results of the Light-Weight Steels

Steel	Yield Strength (MPa)	Tensile Strength (MPa)	Elongation (Pct)	Yield Ratio (Pct)
C1	447	541	0.8	83
C2	576	730	2.6	79
C3	628	836	2.6	75

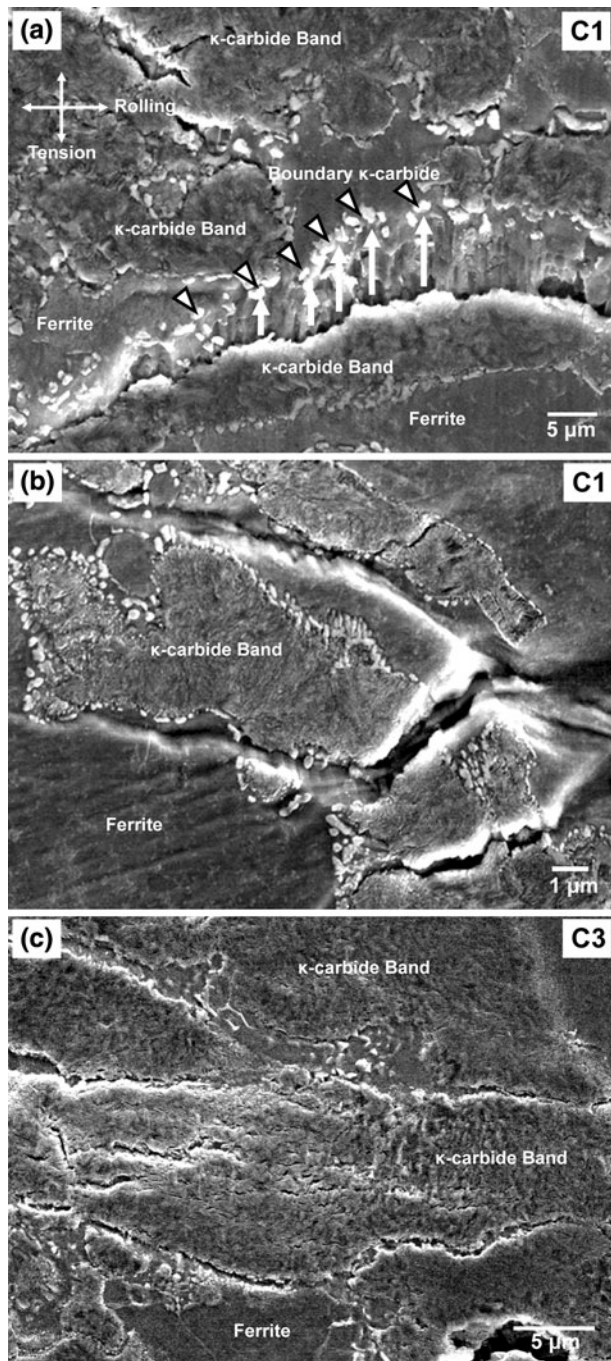


Fig. 7—SEM micrographs of the cross-sectional area beneath the tensile fracture surface of the (a) and (b) C1 steel and (c) C3 steel. Nital etched.

boundaries are also cracked, but this cracking is not serious in comparison to the case of the C1 steel.

Figures 8(a) through (c) show SEM fractographs of the fractured tensile specimens. Since the cracking of band boundary carbides and the subsequent cleavage fracture into ferrites or band boundaries occur in the C1 steel, the fracture takes place mainly by a cleavage fracture mode (Figure 8(a)). Deep and long secondary cracks are well developed (arrow marks) by the cracking

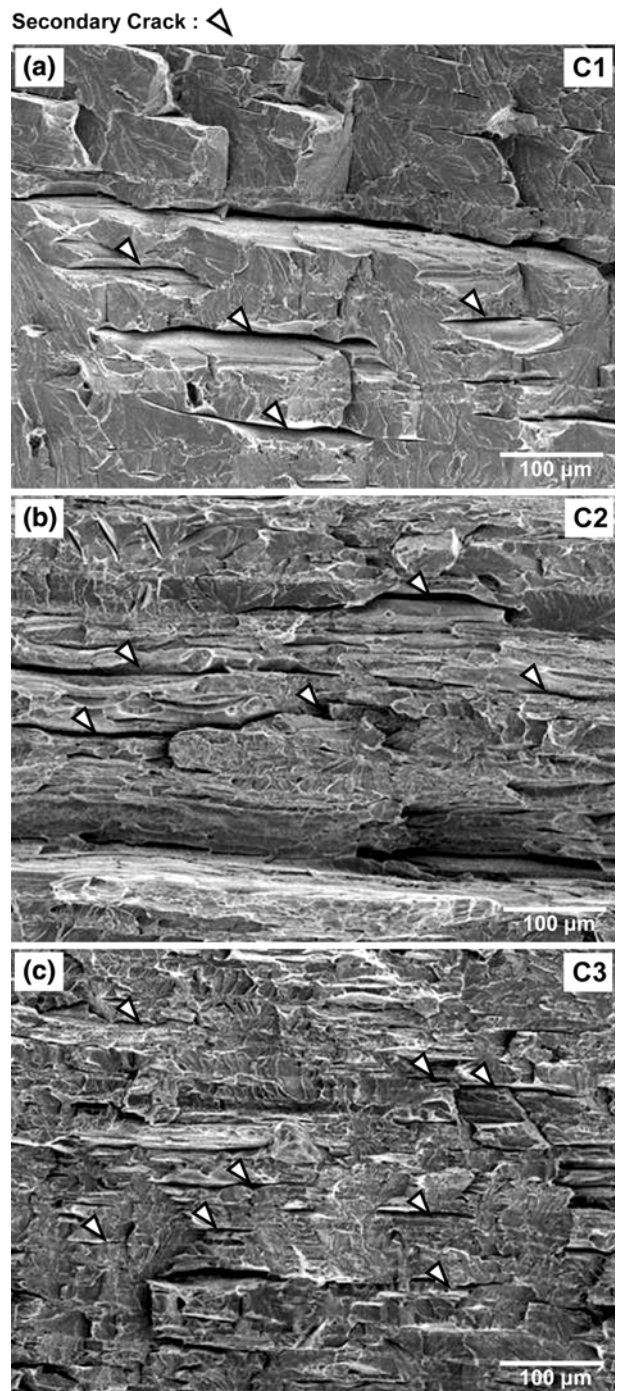


Fig. 8—SEM fractographs of tensile specimens of the (a) C1, (b) C2, and (c) C3 steels.

along band boundary carbides, the crack propagation into band boundaries, and the separation of band boundaries. In the C2 steels, the fracture occurs in a mixed mode of cleavage fracture and quasi-cleavage fracture, and a considerable number of secondary cracks are observed on the fracture surface (Figure 8(b)). In the carbide band areas, the fractured surface looks rather rough to form quasi-cleavage fracture facets, as the cleavage fracture is interrupted by finely dispersed

κ -carbides. In the C3 steel, the quasi-cleavage fracture mode is predominant, while a small amount of cleavage fracture of band boundary carbides is found (Figure 8(c)). Secondary cracks are also observed, but are short and shallow.

IV. DISCUSSION

During cold rolling of light-weight steels, the rolled steel plates are often cracked. Microstructures of the steels are basically composed of ferrite grains and κ -carbides, but the size, morphology, volume fraction, and distribution of κ -carbides are different in the steels. These differences arise mainly from hot-rolling conditions and alloying elements such as carbon. In this study, the cracking phenomenon was analyzed, and the analysis results are discussed in detail as follows.

The C1 steel consists mostly of thin κ -carbide bands, coarse band boundary κ -carbides, and ferrites. According to the observation of the deformed area beneath the fracture surface of the tensile specimen (Figures 7(a) and (b)), the most critical microstructural parameter affecting the cracking is κ -carbides coarsely formed along κ -carbide band boundaries, whereas ferrites or κ -carbide bands do not affect the cracking much. At these coarse band boundary carbides, the deformation is first concentrated to form voids when the tensile stress is applied. These voids are grown to microcracks, which readily propagate along band boundaries to form long and wide cracks. Since the κ -carbide band is densely populated with fine, lamellar κ -carbides, it is hardly cracked. Thus, coarse κ -carbides continuously formed along band boundaries work to initiate the cracking or to facilitate the abrupt crack propagation into ferrites or band boundaries in a cleavage fracture mode. The SEM fractograph in Figure 8(a) shows that the fracture takes place mainly by a cleavage fracture mode, and that deep and long secondary cracks formed by the cracking and separation of band boundaries are observed. Based on these results, band boundary carbides act as crack initiation sites under a tensile load, thereby leading to the very low tensile ductility of 0.8 pct, which is 3 times lower than that of the C2 or C3 steel. The yield and tensile strengths are quite low as the tensile specimen is not sufficiently deformed because cracks initiate and propagate even under a relatively low load.

The C1 steel containing a number of coarse κ -carbides is vulnerable to the cracking. Particularly, when these κ -carbides are populated continuously along band boundaries, cracks can initiate and propagate more easily. The effect of coarse band boundary κ -carbides on the cracking or fracture can be explained by applying a weakest link theory model.^[28] From the perspective of the theory of the weakest link of a chain, the fracture probability (P_{fr}) of κ -carbides can be expressed as

$$P_{fr} = 1 - \exp \left\{ - \left(\frac{d}{\bar{d}} \right)^3 \left(\frac{\bar{d}}{d_N} \right)^3 \left(\frac{\sigma - \sigma_{\min}}{\sigma_0 - \sigma_{\min}} \right)^m \right\} \quad [1]$$

where d refers to particle size, σ to tensile stress acting on particles, σ_{\min} to minimum fracture stress of

particles, m to Weibull inhomogeneity factor, and σ_0 and d_N to normalizing parameters. Equation [1] indicates that the fracture probability of κ -carbides increases with increasing their size (d). As the number and size of κ -carbides increase, the fracture probability at these carbides increases. The probability further increases when κ -carbides are continuously linked, because they can be considered as one long carbide. Thus, in order to prevent the cracking during cold rolling, it is imperative to prevent or minimize the formation of coarse κ -carbides formed along band boundaries.

The formation of band boundary carbides can be reduced by controlling alloying elements and hot rolling conditions. Changing the hot rolling conditions influences the microstructure including κ -carbides, but the control of alloying elements such as carbon is more desirable and simpler, considering the complexity of microstructural changes during hot rolling. For example, when the carbon content increases from 0.1 to 0.3 pct, a considerable amount of carbides are formed, and most of them are placed in a lamellar shape inside the carbide band. In the C3 steel, κ -carbide bands are thick, and band boundary κ -carbides are finely distributed in relatively wide band boundary areas (Figure 5(d)), unlike in the C1 steel. When the tensile load is applied, more microcracks initiate at lamellar carbide/ferrite interfaces inside the thick κ -carbide band than at band boundaries, as the interspacing between lamellar carbides is larger than that of the C1 steel (Figure 7(c)). However, they are not grown further because of the existence of ductile ferrite matrix inside the band. Figure 9 shows an SEM micrograph of the hot-rolled plate of the C3 steel. There are some ferrite areas, which do not contain lamellar carbides, inside the band, and they can prevent the propagation of microcracks during tensile loading or cold rolling. The crack initiation also occurs at band boundaries, but the separation between band boundaries is hardly found because band boundary κ -carbides are finely distributed in the relatively broad band boundary area. According to the fractograph in Figure 8(c), the fracture occurs mainly by a quasi-cleavage mode, in which rough and

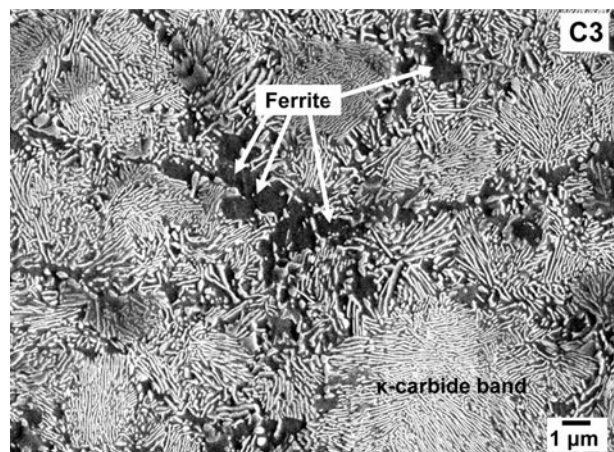


Fig. 9—SEM micrograph of the hot-rolled plate of the C3 steel, showing ductile ferrite inside the κ -carbide band. Nital etched.

fine fracture facets are typically shown, together with a small amount of cleavage fracture at band boundaries. Thus, as in the C3 steel, the increase in carbon content effectively prevents the formation of band boundary carbides and reduces their size, while the formation of the thick carbide band is promoted. Under tensile loading or cold rolling, thick carbide bands are less vulnerable to the cracking than band boundary carbides, and thereby result in the improvement of ductility, which leads to the increase in strength simultaneously, because the tensile specimen or hot-rolled plate is sufficiently deformed up to a considerably high level of stress.

It is interesting to note that the C3 steel containing higher carbon content has higher strength and ductility than the C1 steel containing lower carbon content, which is opposite to the general trend that the strength increases, while the ductility decreases, with increasing carbon content. In fact, the volume fraction of carbide bands composed of fine, lamellar carbides densely distributed in the ferrite matrix is much higher in the C3 steel than in the C1 steel (Table II), but the carbide band seems to have a considerable resistance to cracking, like pearlites in conventional plain-carbon ferrite-pearlite steels. Lee *et al.*^[29] investigated the primary cause for cracking occurring during cupping of a conventional SG295 steel (composition: 0.134C-0.82Mn-0.29Si-0.017P-0.002S-0.032Al-0.0059N) of ferrite-pearlite microstructure. When external stresses were applied, the strain was markedly localized into carbides distributed along ferrite grain boundaries in an isolated and continuous shape, and microvoids were developed and interconnected to cause the grain boundary fracture. The pearlite structure did not significantly influence the cracking, because it was densely populated with lamellar cementites. This result implies that lamellar carbides such as κ -carbides inside bands or cementites inside pearlite grains are hardly cracked if they are densely populated inside a certain area. When κ -carbides or cementites are formed in an isolated shape or a continuous string shape along any boundaries, they are readily voided or cracked to work as preferential sites for cracking. In the C1 steel containing a number of band boundary carbides, therefore, the cracking can frequently occur during cold rolling, although the volume fraction of carbide bands or total carbides is much lower than in the C3 steel.

As the carbon content in the light-weight steels decreases to 0.1 pct, cracks often occur on cold-rolled steel plates. The C1 steel was cracked during cold rolling because κ -carbides precipitated coarsely between bands caused the cracking and the subsequent cleavage fracture. On the other hand, the C3 steel containing a large amount of thick carbide bands was not cracked as band boundary κ -carbides were finely and discontinuously precipitated in the band boundary area, while thick carbide bands hardly influenced the cracking. Thus, it is recommended that the carbon content should be maintained above 0.2 pct at least to precipitate fine, discontinuous band boundary carbides. In the present study, however, hot rolling conditions were not investigated to control the amount and morphology of band carbides,

although the effective reduction in band boundary carbides and the change in carbide shape can be practical methods to improve the resistance to cracking. Therefore, systematic studies on phase-transformation mechanisms involved in local microstructural change during hot rolling as well as microstructural analysis of the primary causes for cracking phenomena are still required, and may indeed be considered as important analytic works for future rolling procedures.

V. CONCLUSIONS

In the present study, the cracking phenomenon occurring during cold rolling of three light-weight steels was clarified in relation to microstructure.

1. Microstructures of the steels were basically composed of ferrite grains and κ -carbides, but the size, morphology, volume fraction, and distribution of κ -carbides were different. The C1 steel consisted mostly of thin κ -carbide bands, coarse band boundary κ -carbides, and ferrites. As the carbon content increased, volume fractions of κ -carbide bands and total κ -carbides increased, while band boundary κ -carbides were finely distributed in relatively wide band boundary areas.
2. Microstructural observation of the deformed region of tensile specimens revealed that κ -carbides formed along band boundaries caused the cracking by forming voids and cracks, while bands densely populated with κ -carbides did not play a critical role in the crack formation. Particularly in the C1 steel, coarse κ -carbides continuously formed along band boundaries worked to initiate the cracking or to facilitate the abrupt crack propagation into ferrites or band boundaries in a cleavage fracture mode.
3. The increase in carbon content effectively prevented the formation of band boundary carbides and reduced their size, while the formation of thick carbide bands was promoted. Under tensile loading or cold rolling, thick carbide bands were less vulnerable to the cracking than band boundary carbides, and thereby resulted in the prevention of the cracking during cold rolling and in the simultaneous improvement of ductility and strength.

ACKNOWLEDGMENTS

This work was supported by POSCO under Contract No. 2008Y221. The authors thank Professor Byeong-Joo Lee and Mr. Chang-hyo Seo, POSTECH, for their help with the alloying effect and microstructural analysis.

REFERENCES

1. K. Sipsos, L. Remy, and A. Pineau: *Metall. Mater. Trans. A*, 1976, vol. 7A, pp. 857–64.
2. L. Remy and A. Pineau: *Mater. Sci. Eng.*, 1977, vol. A28, pp. 99–107.

3. O. Bouaziz and N. Guelton: *Mater. Sci. Eng.*, 2001, vol. A319, pp. 246–49.
4. G. Frommeyer and J.A. Jiménez: *Metall. Mater. Trans. A*, 2005, vol. 36A, pp. 295–300.
5. G. Frommeyer, U. Brück, and P. Neumann: *ISIJ Int.*, 2003, vol. 43, pp. 438–46.
6. Y.W. Kim, N. Kang, Y. Park, I. Choi, G. Kim, S. Kim, and K. Cho: *Kor. J. Met. Mater.*, 2008, vol. 46, pp. 780–88.
7. B.-W. Choi, D.-H. Seo, and J.-I. Jang: *Met. Mater. Int.*, 2009, vol. 15, pp. 373–78.
8. Y. Kimura, K. Handa, K. Hayashi, and Y. Mishima: *Intermetallics*, 2004, vol. 12, pp. 607–17.
9. A. Perlade and P. Maugis: *Discussion Meeting in the Development of Innovative Iron Al Alloys*, Arcelor Research, Toulouse, France, 2005.
10. J.M. Jang, S.J. Kim, N.H. Kang, K.M. Cho, and D.W. Suh: *Met. Mater. Int.*, 2009, vol. 15, pp. 909–16.
11. O. Grässel and G. Frommeyer: *Mater. Sci. Technol.*, 1998, vol. 14, pp. 1213–16.
12. O. Grässel, L. Krüger, G. Frommeyer, and L.W. Meyer: *Int. J. Plast.*, 2000, vol. 16, pp. 1391–1409.
13. Z. Tang and W. Strumpf: *Mater. Character.*, 2008, vol. 59, pp. 717–28.
14. S. Han, H. Seong, Y. Ahn, C.I. García, A.J. DeArdo, and I. Kim: *Met. Mater. Int.*, 2009, vol. 15, pp. 521–29.
15. C. Scott, D. Chaleix, P. Barges, and V. Rebischung: *Scripta Mater.*, 2002, vol. 47, pp. 845–49.
16. R.G. Baligidad, U. Prakash, and A. Radhakrishna: *Mater. Sci. Eng.*, 1998, vol. A255, pp. 162–67.
17. R.G. Baligidad, U. Prakash, A. Radhakrishna, V.R. Rao, P.K. Rao, and N.B. Ballal: *Scripta Mater.*, 1997, vol. 36, pp. 667–71.
18. R.G. Baligidad and A. Radhakrishna: *Mater. Sci. Eng.*, 2000, vol. A287, pp. 17–24.
19. J.H. Chen, G.Z. Wang, C. Yan, H. Ma, and L. Zhu: *Int. J. Fract.*, 1997, vol. 83, pp. 105–20.
20. D.A. Porter and K.E. Easterling: *Phase Transformation in Materials*, 2nd ed., Chapman & Hall, London, 1992, Ch. 4.
21. K. Yamamoto, T. Hasegawa, and J. Takamura: *ISIJ Int.*, 1996, vol. 36, pp. 80–86.
22. Y. Tomita, N. Saito, T. Tsuzuki, Y. Tokunaga, and K. Okamoto: *ISIJ Int.*, 1994, vol. 34, pp. 829–35.
23. U.G. Gang, J.C. Lee, and W.J. Nam: *Met. Mater. Int.*, 2009, vol. 15, pp. 719–25.
24. A.O. Kluken, O. Grong, and J. Hjelen: *Metall. Trans. A*, 1991, vol. 22A, pp. 657–64.
25. K. Wallin, T. Saario, and K. Törrönen: *Int. J. Fract.*, 1987, vol. 32, pp. 201–10.
26. C.Y. Chao and T.F. Liu: *Metall. Mater. Trans. A*, 1993, vol. 23A, pp. 1957–63.
27. P. Kratochvíl: *Intermetallics*, 2009, vol. 17, pp. 39–45.
28. C.A.N. Lanzillotto and F.B. Pickering: *Met. Sci.*, 1982, vol. 16, pp. 371–82.
29. S. Lee, C.G. Lee, D. Kwon, and N.J. Kim: *Metall. Mater. Trans. A*, 1996, vol. 27A, pp. 1241–50.